ACS APPLIED MATERIALS & INTERFACES

Letter

www.acsami.org

DNA Origami-Directed, Discrete Three-Dimensional Plasmonic Tetrahedron Nanoarchitectures with Tailored Optical Chirality

Gaole Dai,[†,‡] Xuxing Lu,[‡] Zhong Chen,[‡] Chun Meng,*[,†] Weihai Ni,*[,‡] and Qiangbin Wang*[,‡]

[†]College of Biological Science and Engineering, Fuzhou University, Fuzhou 350108 China

[‡]Key Laboratory for Nano-Bio Interface Research, Suzhou Key Laboratory for Nanotheranostics, Division of Nanobiomedicine and i-Lab & Collaborative Innovation Center of Suzhou Nano Science and Technology, Suzhou Institute of Nano-Tech and Nano-Bionics, Chinese Academy of Sciences, Suzhou 215123 China

Supporting Information

ABSTRACT: Discrete, three-dimensional (3D) gold nanoparticle (AuNP) tetrahedron nanoarchitectures are successfully self-assembled with DNA origami as template with high purity (>85%). A distinct plasmonic chiral response is experimentally observed from the AuNP tetrahedron nanoarchitectures and appears in a configuration-dependent manner. The chiral optical properties are then rationally engineered by modifying the structural parameters including the AuNP size and interparticle distance. Theoretical study of the AuNP tetrahedron nanoarchitectures shows the dependence of the chiral optical property on the AuNP size and interparticle distance, consistent with the ensemble averaged measurements.

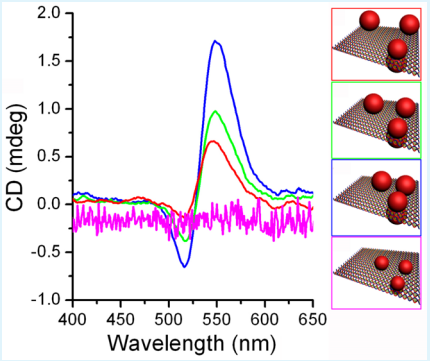

KEYWORDS: *DNA self-assembly, gold nanoparticle, tetrahedron nanostructure, chiral optical property*

Structural DNA nanotechnology has been widely employed for building nanostructures with nanoscale resolution because of the sequence programmability and structural rigidity of DNA molecule. Much progress has been achieved recently in the DNA-programmed self-assembly of nanoarchitectures comprising nano-building blocks, including noble metal nanoparticles,[1−3] semiconductor nanocrystals,[4] and organic dyes.[5,6] As early in 1996, Alivisatos pioneered the discret nanostructures self-assembly directed by DNA, in which one dimensional (1D) gold nanoparticle (AuNP) dimers were complished through hybridizing complementary DNA mono-functionalized AuNPs for the first time.[7] Subsequently, many more complicated two dimensional (2D),[8−10] and three dimensional (3D)[11,12] nanoarchitectures were successfully assembled using DNA as scaffold. These nanoarchitectures give rise to a rich variety of optical properties, such as surface enhanced raman scattering (SERS),[13] surface plasmonic resonance (SPR)[14] and so on.

Recently, chirality of plasmonic nanoarchitectures has been a hot topic in optical properties study. Constructing discrete, asymmetric nanoarchitectures and rational tailoring their plasmonic circular dichroism (CD) are of great significance in understanding their underlying optical interactions. Liedl and coworkers used a 24-DNA helix bundle to direct the positioning of AuNPs, in which helically arranged attachment sites were displayed on the bundle and the helically arranged AuNPs presented chiral optical response.[15] Wang and cow-orkers delicately constructed 3D Au nanorod (AuNR) dimers using a simple bifacial DNA origami as template.[16] Strong chiral optical signals were observed from 'L'-shaped asymmetric 3D dimers. More recently, Ding demonstrated a simple asymmetric AuNP tetrahedron model by organizing four nominally identical AuNPs into two asymmetric tetrahedrons with left-handed and right-handed chirality and investigated their chiral optical properties.[17] As we know, the plasmonic chirality of the AuNP tetrahedron is significantly harvested from a localized electromagnetic field at the AuNP interface, which is relevant to the size of the AuNPs and the interparticle distance between the AuNPs. Therefore, in this contribution, we systematically investigate how the size of AuNP and the interparticle distance between AuNPs affect the chiroptical properties by using the simple AuNPs tetrahedron model.

The process of assembling AuNPs into 3D tetrahedrons is schematically illustrated in Figure 1. The rectangular bifacial DNA origami (90 nm × 60 nm × 2 nm) is self-assembled from a long single-stranded M13 viral genomic DNA with a set of ∼200 short staple strands and rationally designed capture strands (see Figure S1 in the Supporting Information for details). Three copies of capture strands were used to precisely dock one single AuNP on the DNA origami. To obtain the 3D AuNP tetrahedrons, three AuNPs were defined on one side of the DNA origami and the fourth AuNP was positioned on the

Received: March 18, 2014
Accepted: April 9, 2014
Published: April 9, 2014

   dx.doi.org/10.1021/am501599f | ACS Appl. Mater. Interfaces 2014, 6, 5388−5392

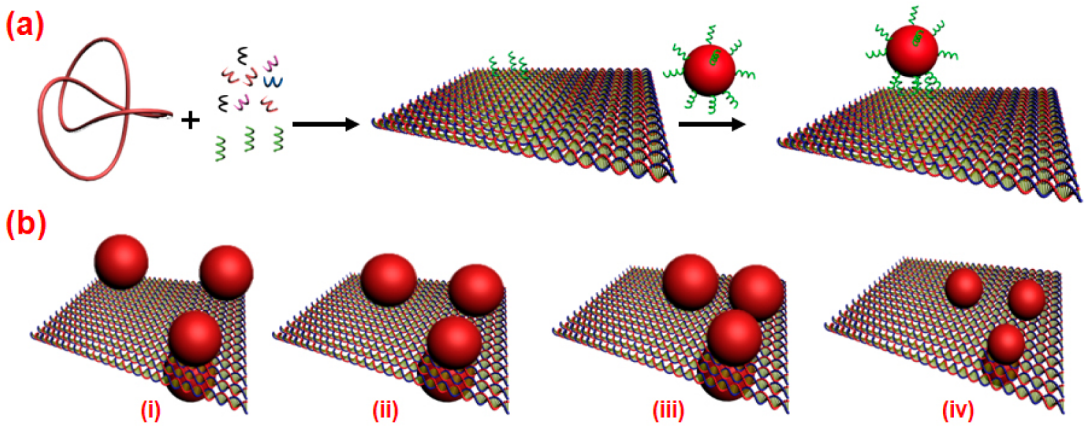

Figure 1. Schematic illustration of (a) a bifacial DNA origami-directed self-assembly of Au AuNP tetrahedrons and (b) the obtained four AuNP tetrahedrons in which (i) 20 nm AuNPs with interparticle distance of 15 nm, (ii) 20 nm AuNPs with interparticle distance of 10 nm, (iii) 20 nm AuNPs with interparticle distance of 5 nm, (iv) 13 nm AuNPs with interparticle distance of 10 nm, respectively.

opposite side, therefore, the interparticle distance between the AuNPs assembled on the two sides of DNA origami is defined to be 12 nm in our study, taking account of the molecule length of two batches of capturing strands and the thickness of origami template. Previous theoretical studies have demonstrated that the particle size and the inter-particle distance can lead to a dramatic interaction of plasmonic resonant coupling among the plasmonic nanoarchitectures and the resultant chiral optical activity.[23−25] Therefore, toward precisely tailoring the plasmonic chirality of discrete AuNP tetrahedrons, we rationally tune the size of AuNPs and the interparticle distance between the three AuNPs on the same side.

The AuNP tetrahedrons were purified from the annealed mixtures by agarose gel electrophoresis. Images a and b in Figure 2 show the agarose gel images (stained by SYBR green) under daylight and UV light, respectively. The sharp bands without smearing indicate the high purity of the products. Lane 1 corresponds to the rectangular DNA origami as reference. Lanes 2− 5 contain the four AuNP tetrahedrons of (i), (ii), (iii), and (iv) illustrated in Figure 1b, respectively. Three gel bands were observed after the electrophoresis of the annealed mixture, in which band A is the free AuNPs in the mixture, band B is the target AuNP tetrahedrons and band C represents the aggregates of AuNPs associated with two or more DNA origami. Due to the much large size of the origami in comparison with the AuNP, AuNP tetrahedrons exhibit approximate mobility compared to the pure DNA origami, whereas the free AuNPs move much faster and the aggregates of AuNPs assocaited with two or more DNA origami move much slower as shown in images a and b in Figure 2. The four target gel bands were then sliced and extracted by electro-elution with dialysis tubing membranes (MWCO 8000−14000). The purified AuNP tetrahedrons were characterized by TEM. As shown in Figure 2c, high purity (>85%) of the designed tetrahedrons was obained. Althogh the relative position of each AuNP in a tetrahedron is difficult to recognize because of the drying process during sampling and the 2D imaging of the samples, the observed structures are in good agreement with their model structures, validating the success of the building the tetrahedrons by using DNA origami directed self-assembly. More TEM images of AuNP tetrahedrons are presented in Figure S2 in the Supporting Information. The high purity of the obtained AuNP tetrahedrons further support the subsequent optical studies of the ensembles.

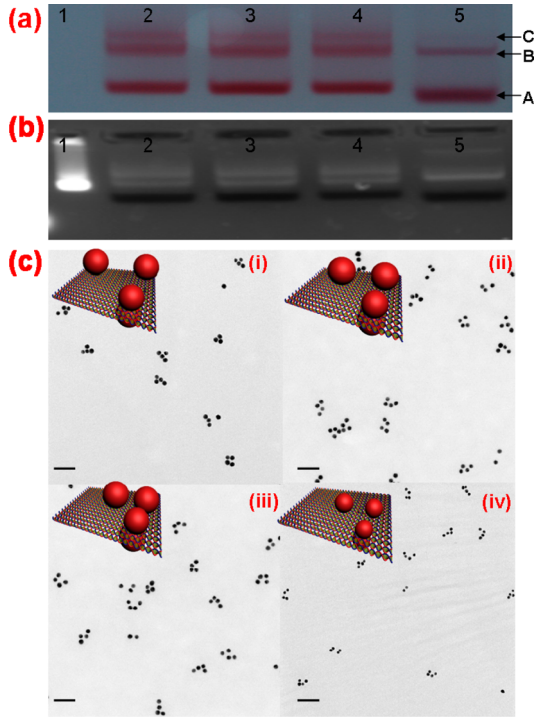

Figure 2. Characterization of the assembled AuNP tetrahedrons. (a) SYBR green-stained agarose gel of the AuNP tetrahedrons assembled on the DNA origami taken under daylight. (b) SYBR green-stained agarose gel of the AuNP tetrahedrons assembled on the DNA origami taken under UV light. Lane 1, the rectangular DNA origami as reference; lanes 2−5 represent the four AuNP tetrahedrons, respectively. (c) TEM images of the obtained AuNP tetrahedrons and their models. All scale bars are 100 nm.

It has been demonstrated that noble metal NPs with localized surface plasmon resonance (LSPR) can generate strong surface electromagnetic fields, which remarkably influence the optical properties of the NP-assembled nanostructures.[18−21] Figure 3a presents the UV−vis spectra of the obtained tetrahedrons. The extinction curve peaks of the tetrahedrons red-shift in comparison with that of the free AuNPs. This is mainly due to the near-field coupling between the AuNPs in the assembled tetrahedrons. Decreasing the interparticle distance leads to a larger red-shift of the extinction

dx.doi.org/10.1021/am501599f | ACS Appl. Mater. Interfaces 2014, 6, 5388−5392

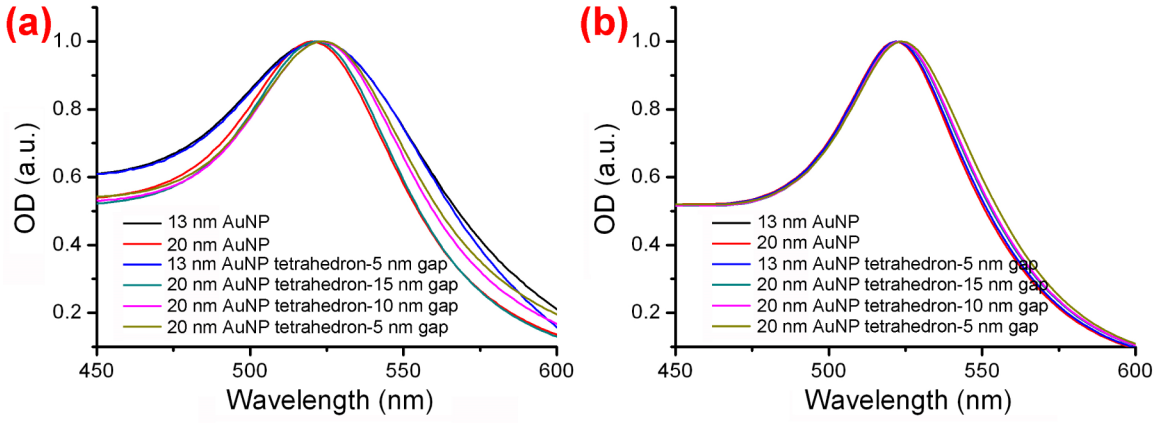

Figure 3. Normalized UV−vis extinction spectra of the four AuNP tetrahedrons: (a) experimental data, (b) calculated data.

spectra because of the stronger coupling among the AuNPs. Figure 3b depicts the calculated results by using coupled dipole approximation (CDA) method. The calculation results qualitatively agree with the experimental data, which further proves high purity of the obtained tetrahedron.

Because of the asymmetry of the prepared AuNP tetrahedrons, CD properties of the tetrahedrons in 1 × TAE/Mg^{2+} buffer solution were measured. The chiral assemblies are oriented along all possible directions with respect to the incident circularly polarized light as they can freely move in water. Figure 4a shows the measured CD spectra of the tetrahedrons. Obviously, the CD spectra of the assembled AuNP tetrahedrons exhibit characteristic bisignate signatures.

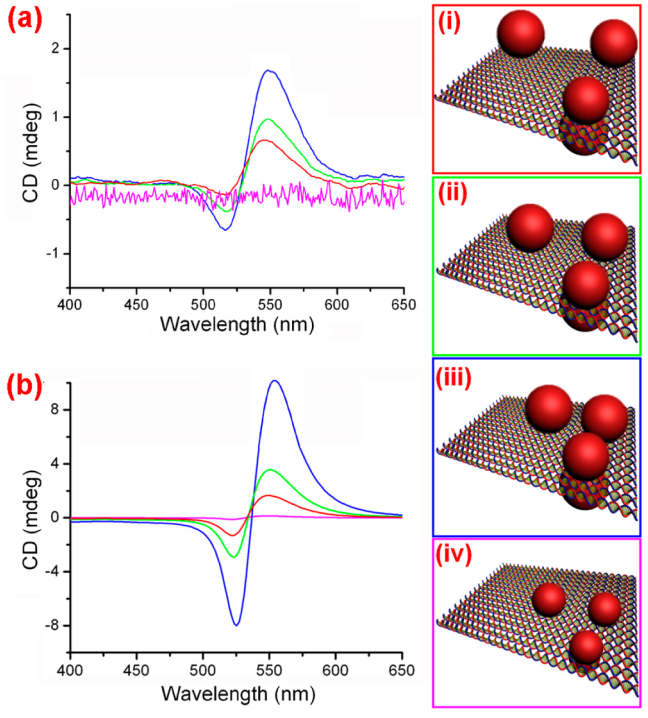

Figure 4. CD spectra of the four AuNP tetrahedrons (a) Experimental data, (b) Calculated results. (i) 20 nm AuNPs with interparticle distance of 15 nm (red curve in a and b), (ii) 20 nm AuNPs with interparticle distance of 10 nm (green curve in a and b), (iii) 20 nm AuNPs with interparticle distance of 5 nm (blue curve in a and b), (iv) 13 nm AuNPs with interparticle distance of 10 nm (magenta curve in a and b).

In a group of tetrahedron consisted of 20 nm AuNPs, the CD signal continually increases with the decrease of the interparticle distance of AuNP from 15 to 10 nm and 5 nm. These results reveal that the interparticle distance of AuNP plays an important role in determining the CD behaviour. Decreasing the size of AuNP from 20 to 13 nm, the CD signal intensities decrease dramatically as shown in Figure 4a. Our ensemble-measured CD spectra clearly demonstrate the size and distance dependence of the CD intensity of AuNP tetrahedrons. The variation of CD signal is completely in conformity with the shift of extinction spectra. Increasing the interparticle distance and decreasing the particle size weaken the interaction among the AuNPs which recedes the plasmonic resonance coupling of the four AuNPs in the tetrahedron. Therefore, to achieve strong chirality in an artificial plasmonic chiral structure, the plasmonic resonant coupling and structural asymmetry are both essential elements.

Toward deep understanding of the plasmonic chirality of the obtained AuNP tetrahedrons, Coupled-dipole approximation (CDA) theoretical calculation is performed to calculate the optical response of the AuNP tetrahedrons. In this model, each particle of the tetramer is approximated as a electric point dipole with a polarization[22]

$$\mathbf{p}_j = \alpha_j \mathbf{E}_j$$

where $\alpha_j = (3V_j/4\pi)((\varepsilon_j - \varepsilon_m)/(\varepsilon_j + 2\varepsilon_m))$ is the polarizability of NP j, V_j is the volume of the particle, $\varepsilon_m = 1.33^2$ is the permittivity of water, $\varepsilon_j$is the Au dielectric function that was taken from the previous report,[23] and $\mathbf{E}_j$ is the electric field at $\mathbf{r}_j$, which can be expressed as the sum of incidence $\mathbf{E}_{\mathrm{inc},j}$ and the contribution from the dipole at $\mathbf{r}_i$

$$\vec{\mathbf{G}}_{j,i}\cdot\mathbf{p}_i = \frac{\exp(ikr_{ji})}{r_{ji}^{3}}\left\{\frac{(1 - ikr_{ji})}{r_{ji}^{2}}[3\mathbf{r}_{ji}(\mathbf{r}_{ji}\cdot\mathbf{p}_i) - r_{ji}^{2}\mathbf{p}_i] - k^2\mathbf{r}_{ji}\times(\mathbf{r}_{ji}\times\mathbf{p}_i)\right\}$$

where $\mathbf{r}_{ji} = \mathbf{r}_j - \mathbf{r}_i$, $r_{ji} = |\mathbf{r}_j - \mathbf{r}_i|$.

Then the coupled equation for dipole $\mathbf{p}_j$ can be written as

$$\sum_{i=1}^{N}(\delta_{j,i}\vec{\mathbf{I}} - \alpha_j\vec{\mathbf{G}}_{j,i})\cdot\mathbf{p}_i = \alpha_j\mathbf{E}_{\mathrm{inc},j}$$

dx.doi.org/10.1021/am501599f | ACS Appl. Mater. Interfaces 2014, 6, 5388−5392

By solving these equations, we get polarization $\mathbf{p}_j$, and the extinction cross section can be expressed as[24]

$$\sigma_{\pm} = \frac{4\pi k}{|\mathbf{E}_{inc}|^2} \sum_{j=1}^{2} \mathrm{Im}(\mathbf{E}^*_{inc,j,\pm} \cdot \mathbf{p}_{j,\pm})$$

The CD of the tetramer can finally be calculated by

$$\sigma_{CD} = \langle \sigma_+ - \sigma_- \rangle_\Omega$$

where $\pm$ denotes the left- and right-handed circular polarization, respectively. $<\cdots>_\Omega$ represents the average over all possible orientations as the NP tetramer is considered randomly oriented in the solution.[25] In our calculation, the averages was carried out by sampling all the possible orientation angles in the three dimension by a step of 10°.

If one considers the concentration of the tetramer in the solution (c = 1 nM) and the length of the optical path (l = 1 mm), the ellipticity can be written in mdeg as

$$\mathrm{CD\ (mdeg)} = 1000 \frac{180}{4\pi} N_a \sigma_{CD} c l$$

Figure 4b shows the calculated CD spectra, which are in a qualitatively good agreement with our experimental tendency of the size and distance impact in the CD properties. Increasing the interparticle distance and decreasing the particle size obviously weaken the CD signal.

In conclusion, we have successfully fabricated a series of AuNPs tetrahedron nanoarchitectures with high purity through DNA origami-directed self-assembly of AuNPs. Varying the size of AuNPs and the location of AuNPs allows us to precisely tune the size and interparticle distance of the obtained AuNPs tetrahedrons, thus engineering the chiral optical properties. The experimental CD response of the ensemble AuNPs tetrahedrons match very well with that of the calculation. Our strategy shows great potentials in future plasmonic chirality studies, for example, the chiral plasmonic ruler, where shifting the location of AuNPs in tetrahedron nanoarchitectures at nanometer scale leads to strong perturbation in plasmonic CD. Also, precise positioning of other optical components, such as quantum dots and fluorescent molecules, onto the surface of the underlying DNA origami template enables coupling to the localized surface plasmon in the assembled plasmonic nanoarchitectures and promises future nanophotonic applications.

■ ASSOCIATED CONTENT

Supporting Information

Experimental sections, DNA sequences, and TEM figures. This material is available free of charge via the Internet at http://pubs.acs.org.

■ AUTHOR INFORMATION

Corresponding Authors

*E-mail: qbwang2008@sinano.ac.cn.
*E-mail: mengchun@fzu.edu.cn.
*E-mail: whni2012@sinano.ac.cn.

Notes

The authors declare no competing financial interest.

■ ACKNOWLEDGMENTS

We acknowledge funding by Chinese Academy of Sciences "Bairen Ji Hua" program, the Ministry of Science and Technology (Grant 2011CB965004), the National Natural Science Foundation of China (Grant 21303249, 21301187), the Natural Science Foundation of Jiangsu Province (Grant BK2012007), and the CAS/SAFEA International Partnership Program for Creative Research Teams.

■ REFERENCES

(1) Mastroianni, A. J.; Claridge, S. A.; Alivisatos, A. P. Pyramidal and Chiral Groupings of Gold Nanocrystals Assembled using DNA Scaffolds. *J. Am. Chem. Soc.* **2009**, *131*, 8455−8459.

(2) Lan, X.; Chen, Z.; Liu, B. J.; Ren, B.; Henzie, J.; Wang, Q. DNA-Directed Gold Nanodimers with Tunable Sizes and Interparticle Distances and Their Surface Plasmonic Properties. *Small* **2013**, *9*, 2308−2315.

(3) Sharma, J.; Chhabra, R.; Cheng, A.; Brownell, J.; Liu, Y.; Yan, H. Control of Self-Assembly of DNA Tubules through Integration of Gold Nanoparticles. *Science* **2009**, *323*, 112−116.

(4) Fu, A.; Micheel, C. M.; Cha, J.; Chang, H.; Yang, H.; Alivisatos, A. P. Discrete Nanostructures of Quantum Dots/Au with DNA. *J. Am. Chem. Soc.* **2004**, *126*, 10832−10833.

(5) Du, K.; Ko, S. H.; Gallatin, G. M.; Yoon, H. P.; Liddle, J. A.; Berglund, A. J. Quantum Dot-DNA Origami Binding: a Single Particle, 3D, Real-Time Tracking Study. *Chem. Commun.* **2013**, *49*, 907−909.

(6) Deng, Z.; Samanta, A.; Nangreave, J.; Yan, H.; Liu, Y. Robust DNA-Functionalized Core/Shell Quantum Dots with Fluorescent Emission Spanning from UV−vis to Near-IR and Compatible with DNA-Directed Self-Assembly. *J. Am. Chem. Soc.* **2012**, *134*, 17424−17427.

(7) Alivisatos, A. P.; Johnsson, K. P.; Peng, X.; Wilson, T. E.; Loweth, C. J.; Bruchez, M. P.; Schultz, P. G. Organization of'Nanocrystal Molecules using DNA. *Nature* **1996**, *382*, 609−611.

(8) Wen, Y.; McLaughlin, C. K.; Lo, P. K.; Yang, H.; Sleiman, H. F. Stable Gold Nanoparticle Conjugation to Internal DNA Positions: Facile Generation of Discrete Gold Nanoparticle−DNA Assemblies. *Bioconjugate Chem.* **2010**, *21*, 1413−1416.

(9) Chen, Z.; Lan, X.; Wang, Q. DNA Origami Directed Large-Scale Fabrication of Nanostructures Resembling Room Temperature Single-Electron Transistors. *Small* **2013**, *9*, 3567−3571.

(10) Sharma, J.; Chhabra, R.; Liu, Y.; Ke, Y.; Yan, H. DNA-Templated Self-Assembly of Two-Dimensional and Periodical Gold Nanoparticle Arrays. *Angew. Chem., Int. Ed.* **2006**, *45*, 730−735.

(11) Yan, W.; Xu, L.; Xu, C.; Ma, W.; Kuang, H.; Wang, L.; Kotov, N. A. Self-Assembly of Chiral Nanoparticle Pyramids with Strong R/S Optical Activity. *J. Am. Chem. Soc.* **2012**, *134*, 15114−15121.

(12) Shen, X.; Song, C.; Wang, J.; Shi, D.; Wang, Z.; Liu, N.; Ding, B. Rolling up Gold Nanoparticle-Dressed DNA Origami into Three-Dimensional Plasmonic Chiral Nanostructures. *J. Am. Chem. Soc.* **2011**, *134*, 146−149.

(13) Lan, X.; Chen, Z.; Lu, X.; Dai, G.; Ni, W.; Wang, Q. DNA-Directed Gold Nanodimers with Tailored Ensemble Surface-Enhanced Raman Scattering Properties. *ACS Appl. Mater. Interfaces* **2013**, *5*, 10423−10427.

(14) Pal, S.; Deng, Z.; Wang, H.; Zou, S.; Liu, Y.; Yan, H. DNA Directed Self-Assembly of Anisotropic Plasmonic Nanostructures. *J. Am. Chem. Soc.* **2011**, *133*, 17606−17609.

(15) Kuzyk, A.; Schreiber, R.; Fan, Z.; Pardatscher, G.; Roller, E.-M.; Högele, A.; Simmel, F. C.; Govorov, A. O.; Liedl, T. DNA-Based Self-Assembly of Chiral Plasmonic Nanostructures with Tailored Optical Response. *Nature* **2012**, *483*, 311−314.

(16) Lan, X.; Chen, Z.; Dai, G.; Lu, X.; Ni, W.; Wang, Q. Bifacial DNA Origami-Directed Discrete, Three-Dimensional, Anisotropic Plasmonic Nanoarchitectures with Tailored Optical Chirality. *J. Am. Chem. Soc.* **2013**, *135*, 11441−11444.

(17) Shen, X.; Asenjo-Garcia, A.; Liu, Q.; Jiang, Q.; García de Abajo, F. J.; Liu, N.; Ding, B. Three-Dimensional Plasmonic Chiral Tetramers Assembled by DNA Origami. *Nano Lett.* **2013**, *13*, 2128−2133.

(18) Feng, M.; Zhang, M.; Song, J.-M.; Li, X.-G.; Yu, S.-H. Ultralong Silver Trimolybdate Nanowires: Synthesis, Phase Transformation,

sStability, and Their Photocatalytic, Optical, and Electrical Properties. *ACS Nano* **2011**, *5*, 6726−6735.
(19) Huang, X.; Neretina, S.; El-Sayed, M. A. Gold Nanorods: from Synthesis and Properties to Biological and Biomedical Applications. *Adv. Mater.* **2009**, *21*, 4880−4910.
(20) Mirkin, C. A. Programming the Assembly of Two-and Three-Dimensional Architectures with DNA and Nanoscale Inorganic Building Blocks. *Inorg. Chem.* **2000**, *39*, 2258−2272.
(21) Zhu, Z.; Meng, H.; Liu, W.; Liu, X.; Gong, J.; Qiu, X.; Jiang, L.; Wang, D.; Tang, Z. Superstructures and SERS Properties of Gold Nanocrystals with Different Shapes. *Angew. Chem.* **2011**, *123*, 1631−1634.
(22) Bohren, C. F.; Huffman, D. R. *Absorption and Scattering of Light by Small Particles*; Wiley−Interscience: New York, 2008.
(23) Johnson, P. B.; Christy, R.-W. Optical Constants of the Noble Metals. *Phys. Rev. B* **1972**, *6*, 4370.
(24) Draine, B. T. The Discrete-Dipole Approximation and Its Application to Interstellar Graphite Grains. *Astrophys. J.* **1988**, *333*, 848−872.
(25) Fan, Z.; Govorov, A. O. Plasmonic Circular Dichroism of Chiral Metal Nanoparticle Assemblies. *Nano Lett.* **2010**, *10*, 2580−2587.